

How Foam Develops Apparent Viscosity in CO₂ EOR

George J. Hirasaki
Rice University

Whole Value Chain CCUS
Golden, CO
November 14-18, 2022

Outline

- **Current state of the art**
- **Choice of surfactant**
- **Smooth capillaries**
- **Effect of constrictions**
- **Foam texture**
- **Mechanisms for foam generation**
- **Mechanisms for foam destruction**
- **Population balance**
- **Minimum pressure gradient for foam generation**
- **Empirical foam model for reservoir simulation**
- **Experiments and simulations for field application**
- **Conclusions**

Current state of the art: Measurements and modeling

Effect of permeability on apparent viscosity

$$\mu_f^{app} \equiv \frac{k}{(u_w + u_g)} \frac{\Delta p}{L}$$

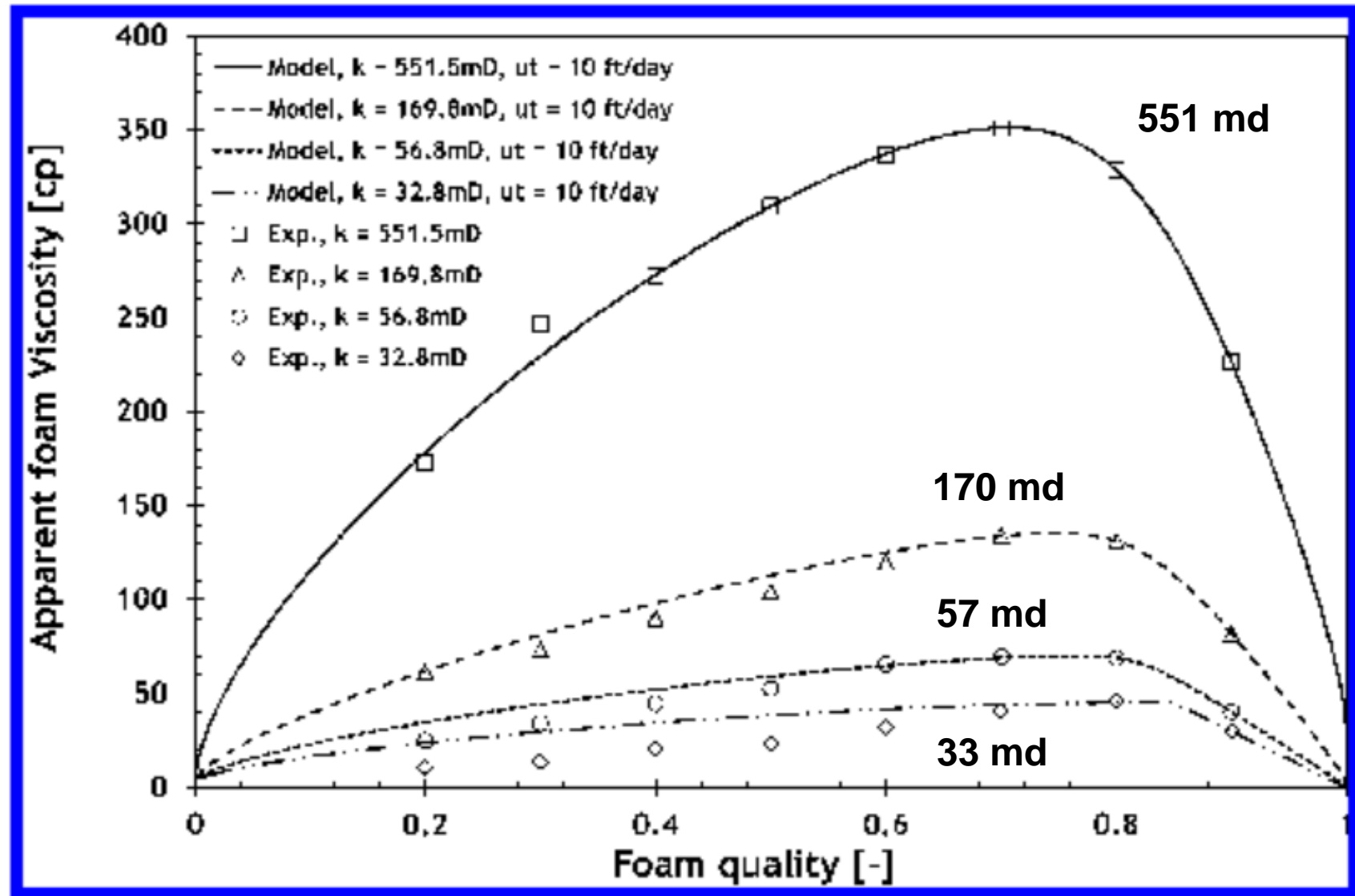


Figure 3. Apparent viscosity of CO₂ foam made with 2000 ppm of Chaser CD-1050 as a function of permeability.

Choice of surfactant

- **Reservoir: sandstone or carbonate, salinity, temperature**
- **Type of surfactant**
 - **Anionic: sulfonate, sulfate, ethoxy- sulfate, ethoxy- carboxylate**
 - **Nonionic: ethoxylated alcohol, glucoside**
 - **Cationic: amine, diamine**
 - **Zwitterionic: betaine, amido-betaine, sulfo-betaine**
- **Carbon number of surfactant, C12 → C18**
- **Low adsorption on formation minerals**
- **Chemical stability**
- **Negligible partition into oil phase**

Elhag, et al., 2014.

Chen, et al., 2015.

Svorstoel, I., et al., 1996.

How does foam gain flow resistance?

Smooth capillaries

Contributors to flow resistance

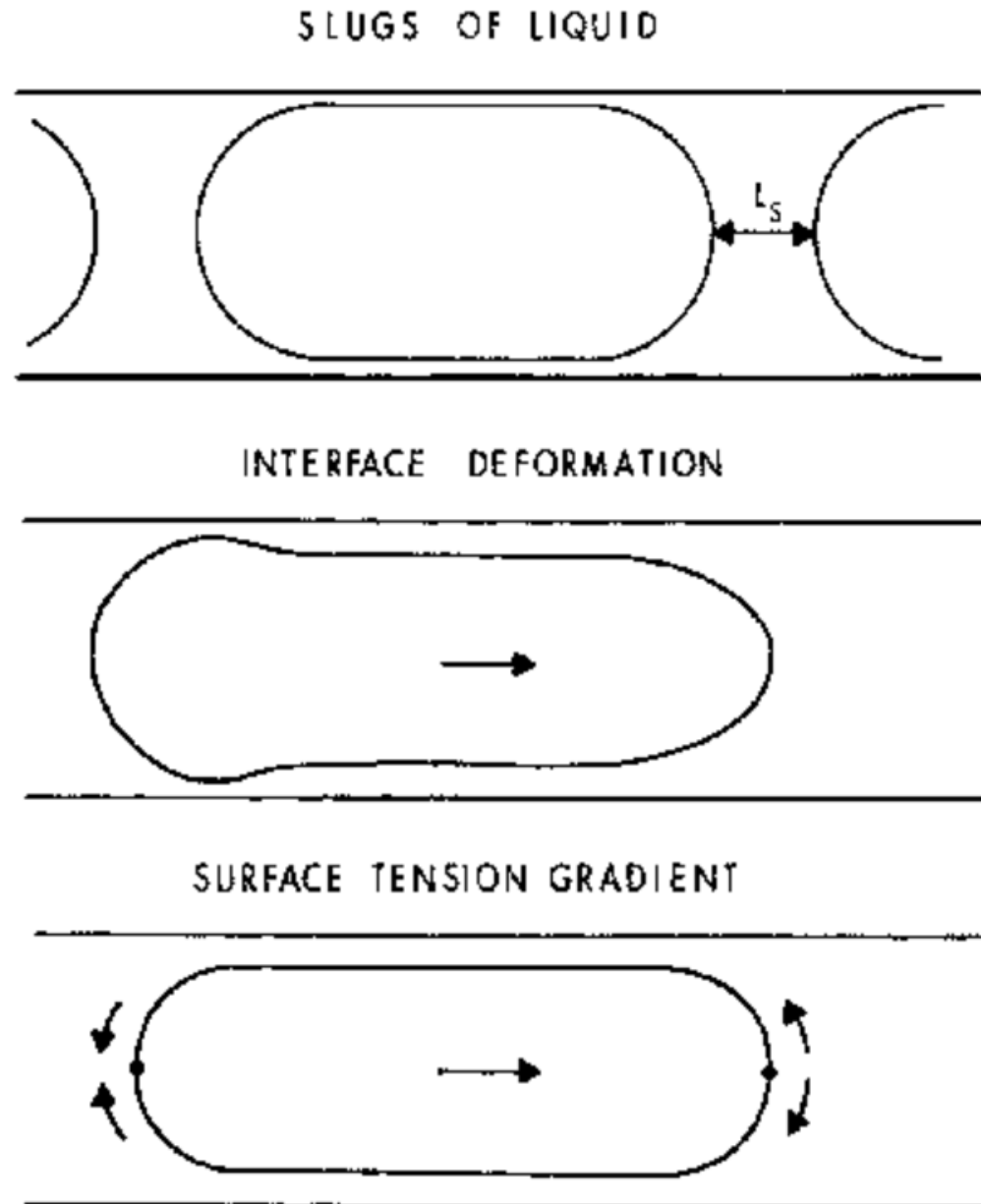


Fig. 1—Mechanisms affecting apparent viscosity in smooth capillaries.

Smooth capillaries

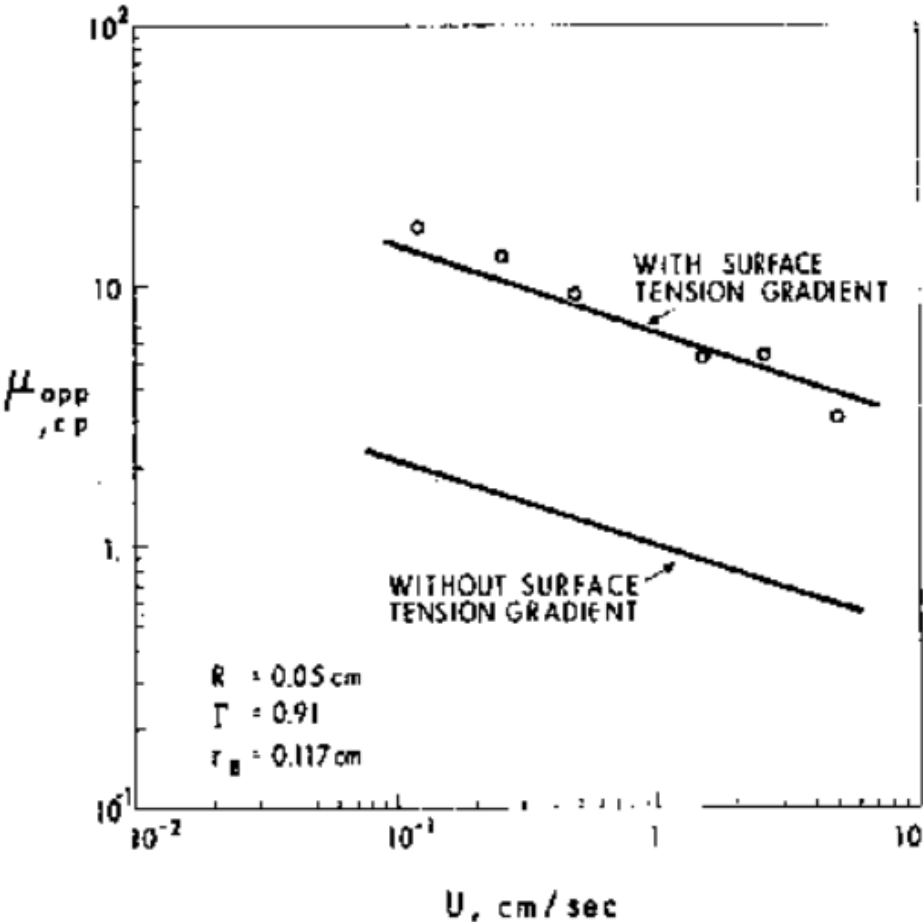
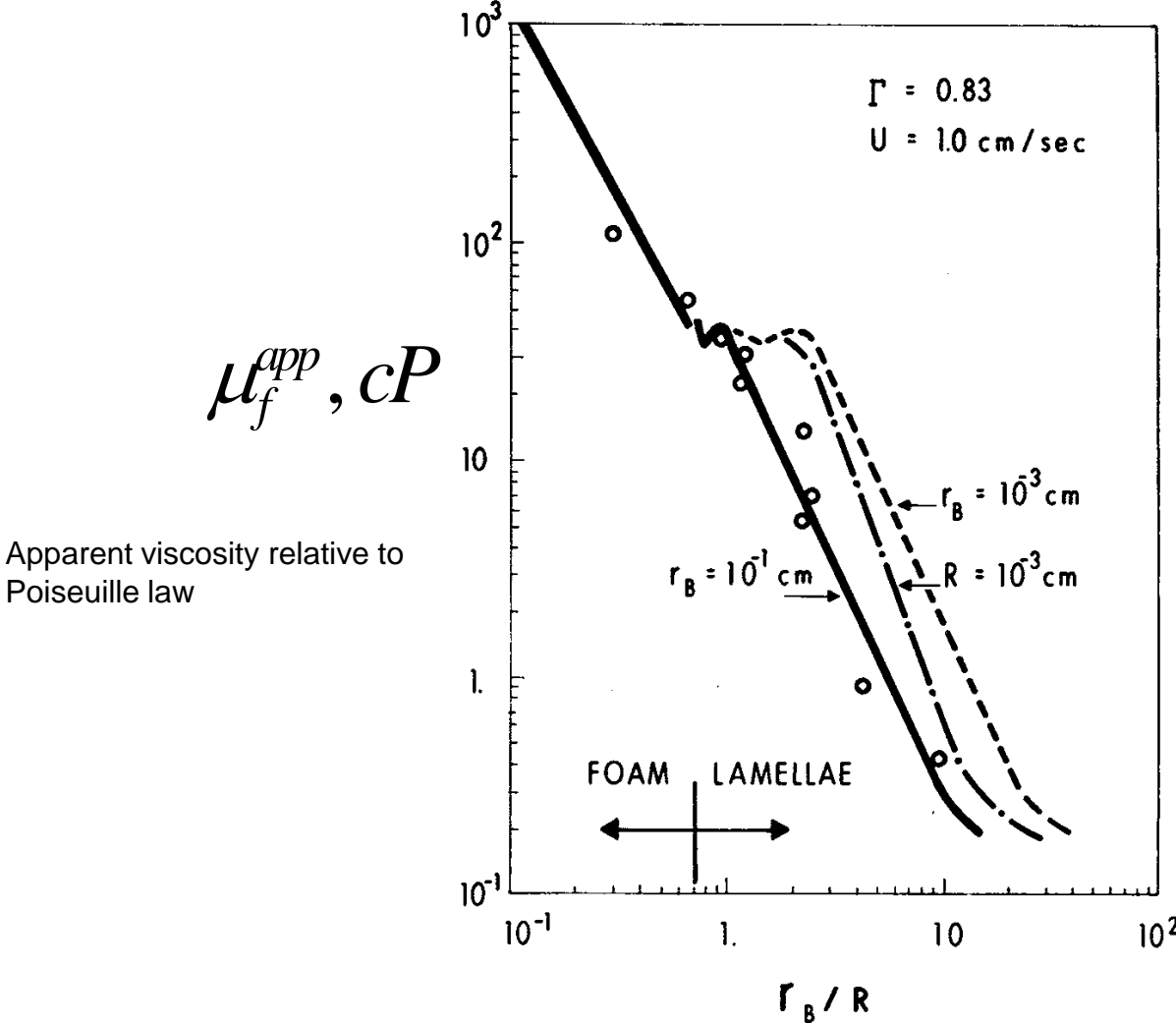


Fig. 10—Effect of surface tension gradient on apparent viscosity.

Hirasaki and Lawson, 1985, *SPEJ*

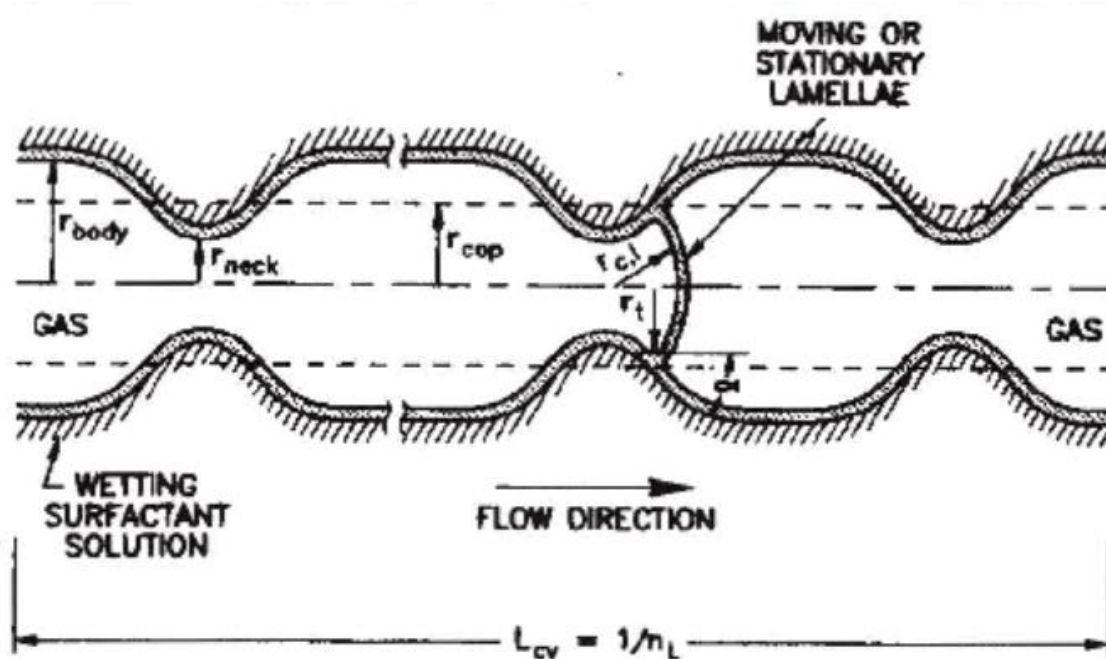


Combined effects of bubble size and capillary radius

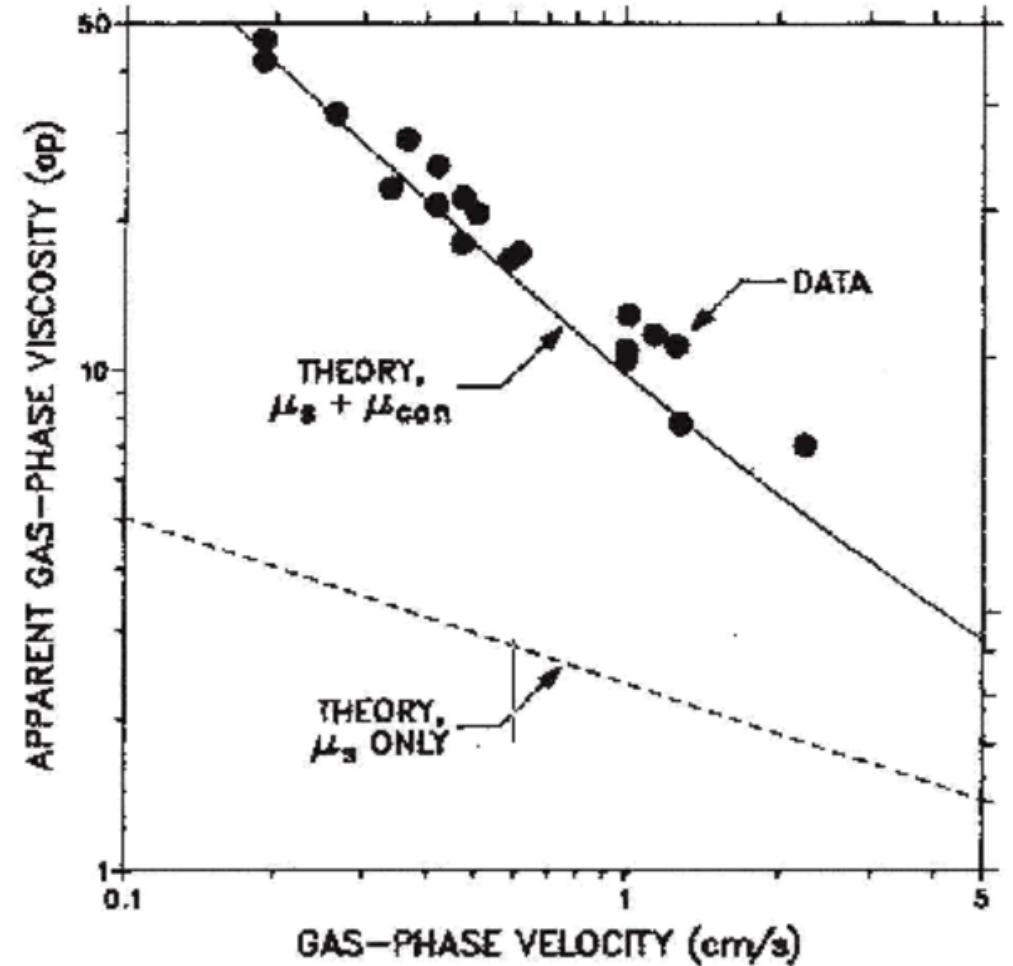
Effect of constrictions

Bubbles in smooth capillaries are power-law fluid.

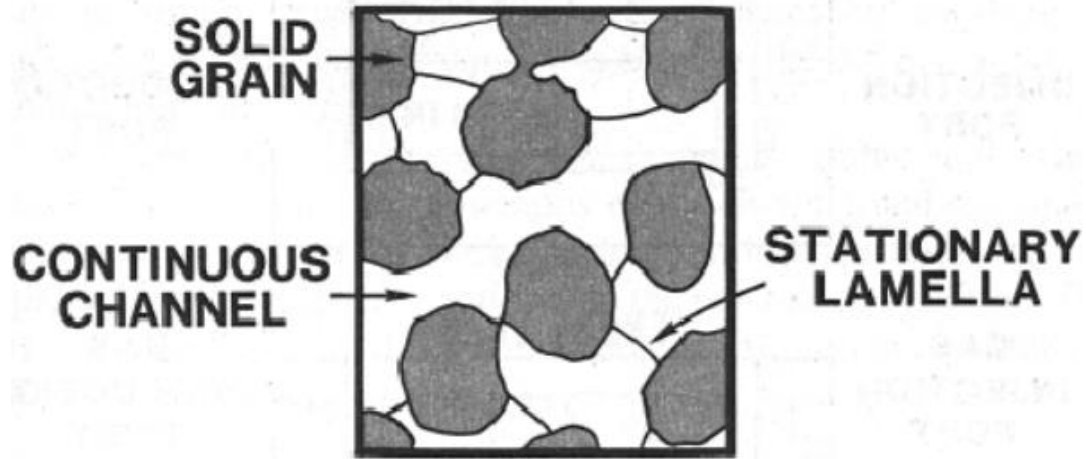
Pore constrictions have increasing effect at lower velocities and result in gas trapping



A.H. Falls, et al., 1989, *SPERE*

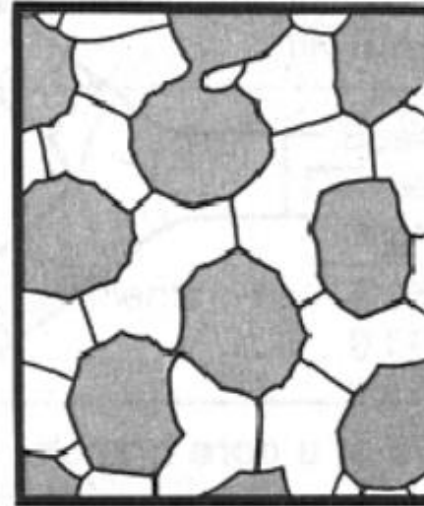


Foam texture

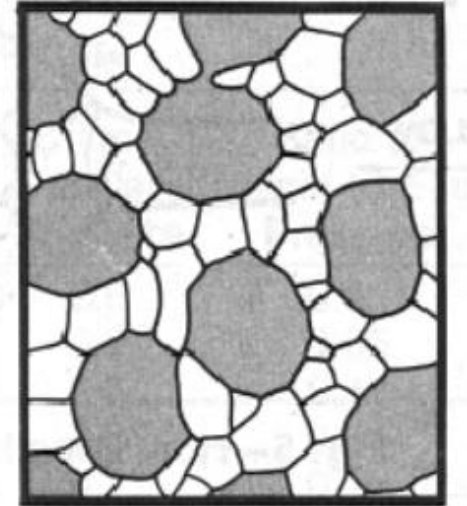


Continuous-gas foam

COARSELY TEXTURED



FINELY TEXTURED



Discontinuous-gas foam

Mechanisms for foam generation

- Bubble or lamella division
 - Branch points in flowing train of bubbles offer opportunity for bubble or lamellae division
 - Responsible for transition from continuous-gas foam to discontinuous-gas foam

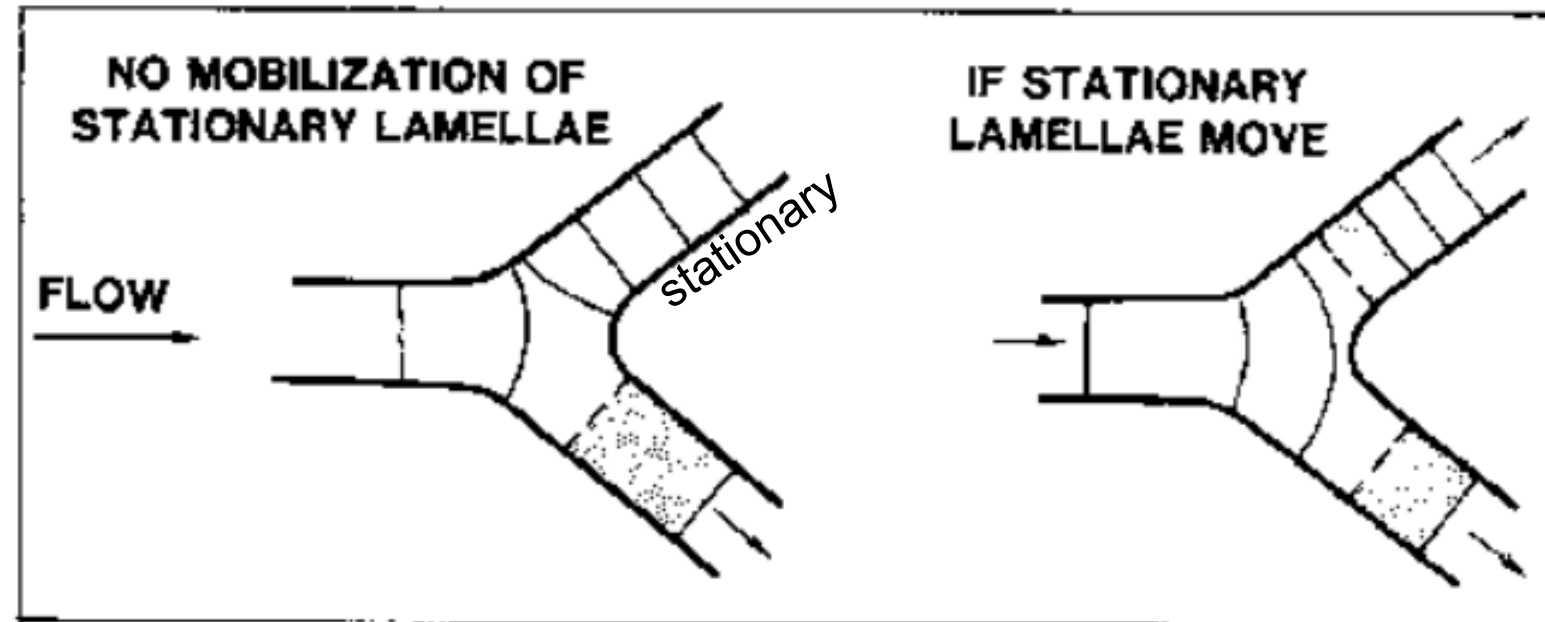


Fig. 5—How lamellae can divide at a pore branch.

Mechanisms for foam generation

- **Capillary snap-off**
 - Pore body/throat contrast and water saturation
 - Permeability contrast and water saturation
 - Spontaneous migration of water from larger to smaller pores
 - Capillary pressure for snap-off is $<$ one-half of capillary entry pressure

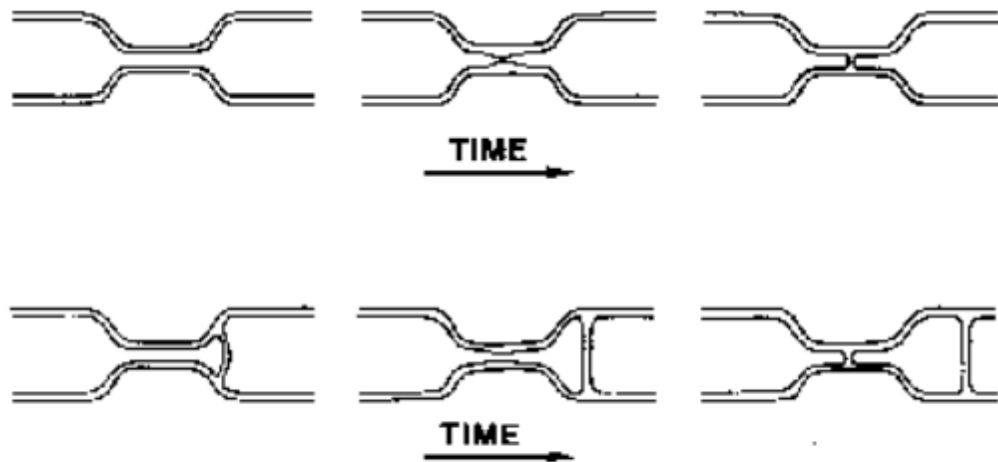


Fig. 4—How capillary snap-off can generate foam lamellae in a constricted capillary tube.

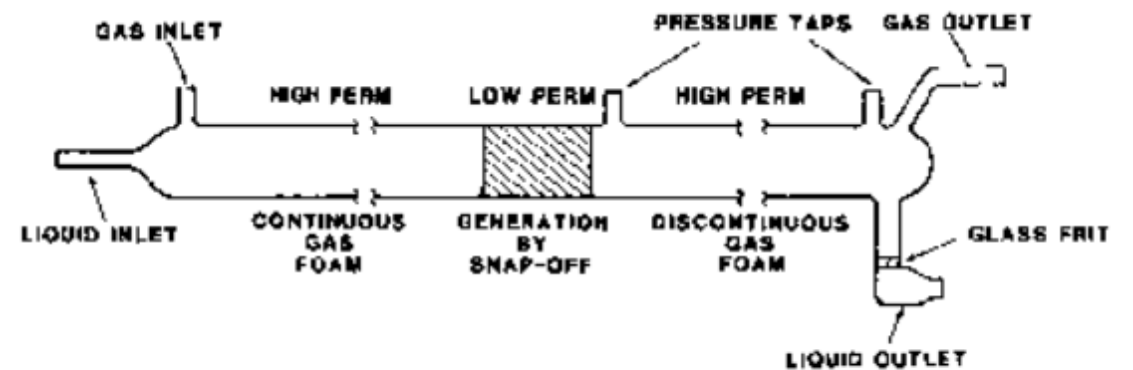


Fig. 7—Bead pack consisting of a low-permeability zone between two sections of higher permeability.

Mechanisms for foam destruction

- Capillary pressure, P_c exceeds maximum stable disjoining pressure. This limits bubble refinement.
- Mass transfer from small bubbles to large bubbles
- Spreading of oil at gas/water interface

Population balance of bubble sizes

- **Flowing and stationary gas bubbles**
- **Size distributions or mean value of bubble size**
- **Bubble density, i.e., number of bubbles per unit volume of gas**
- **Accumulation = -Divergence of flux + generation – destruction**
- **Mass balance for two phase flow**

Population balance

A.H. Falls, et al., 1988,
SPERE, Aug.

Generation only by snap-off

Grain sizes, 4:1

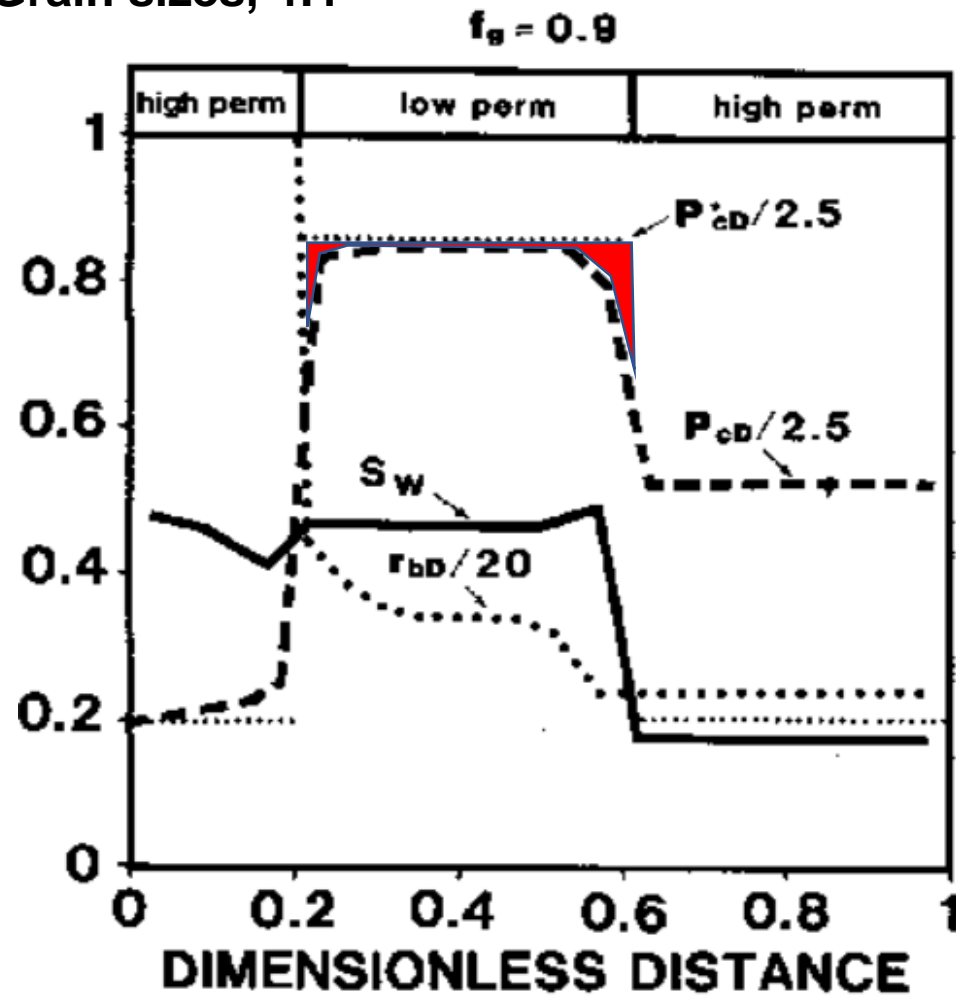


Fig. 9—Profiles of liquid saturation, capillary pressure, and bubble size simulated for $f_g = 0.9$.

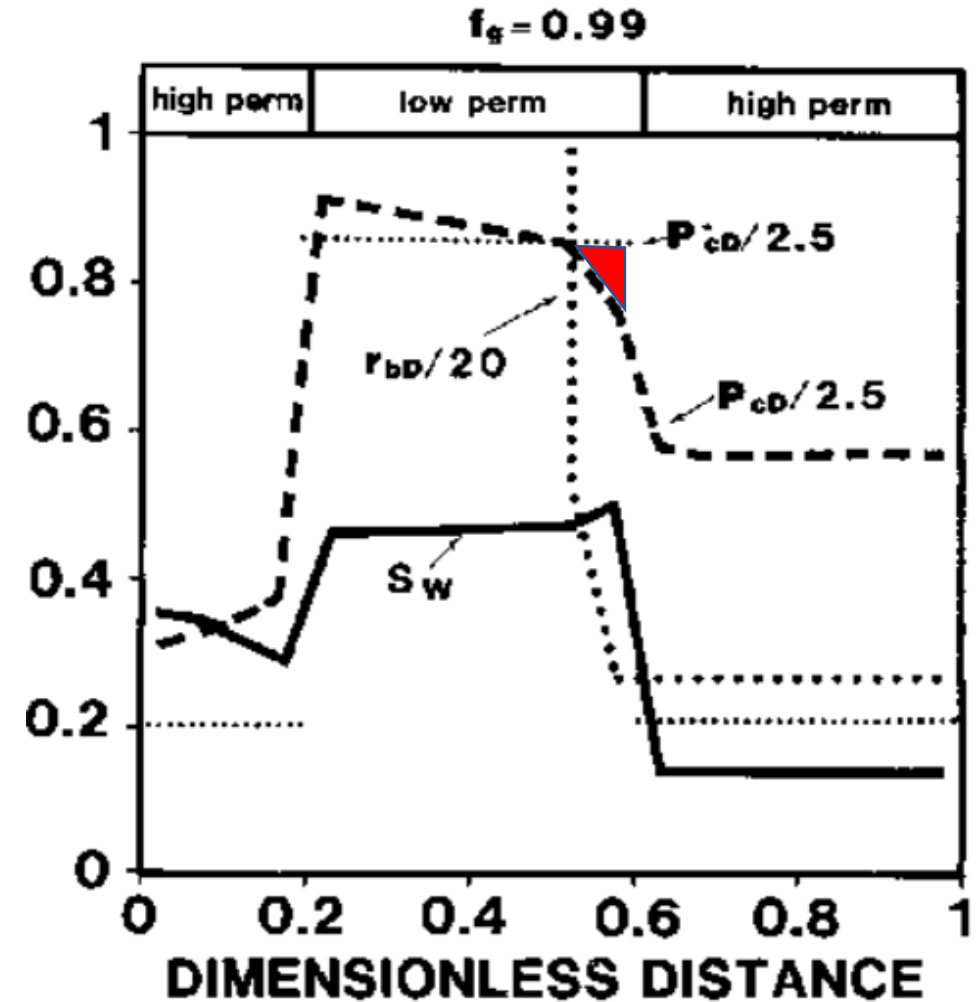


Fig. 8—Simulated profiles of liquid saturation, normalized capillary pressure, and normalized bubble size for $f_g = 0.99$.

Illustration of foam in homogeneous and heterogeneous sandpacks (weakly foaming surfactant for aquifer remediation)

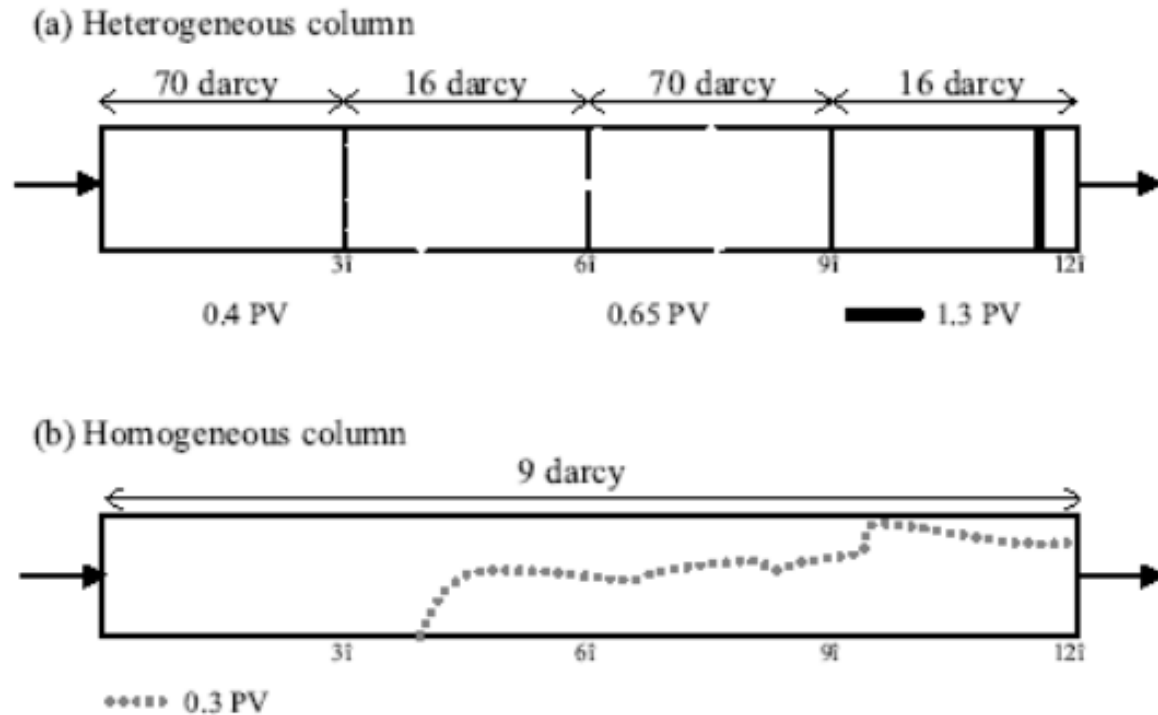


Fig. 11—Location and shape of the gas displacement front during transient foam experiments in (a) heterogeneous column with alternating high and low permeabilities, and (b) homogeneous column with low permeability. $f_g=67\%$ and $u_g=0.6$ ft/day.

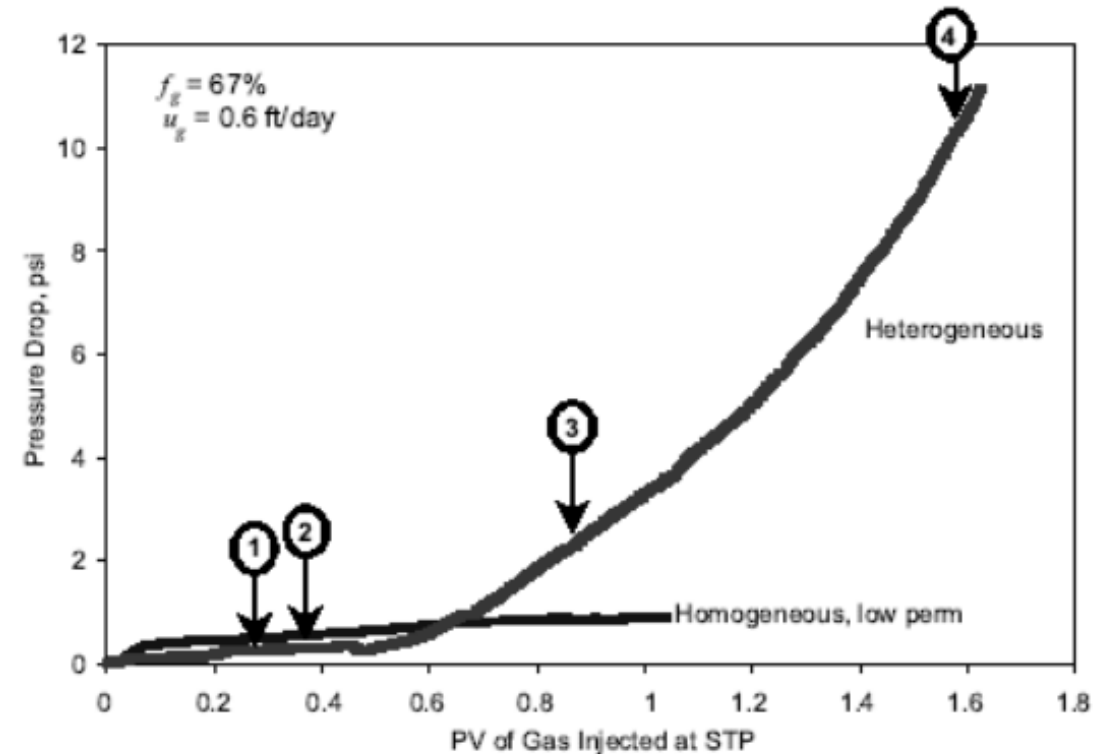
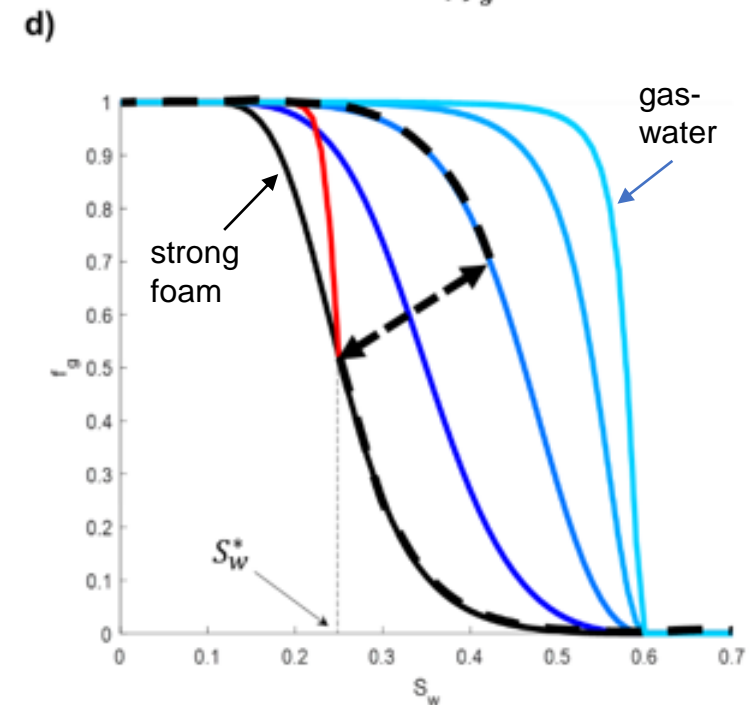
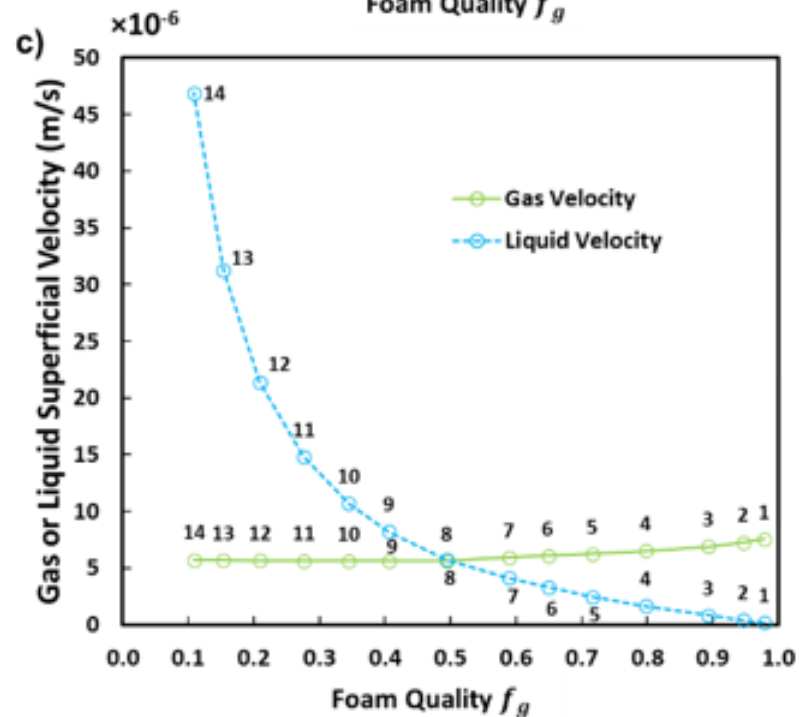
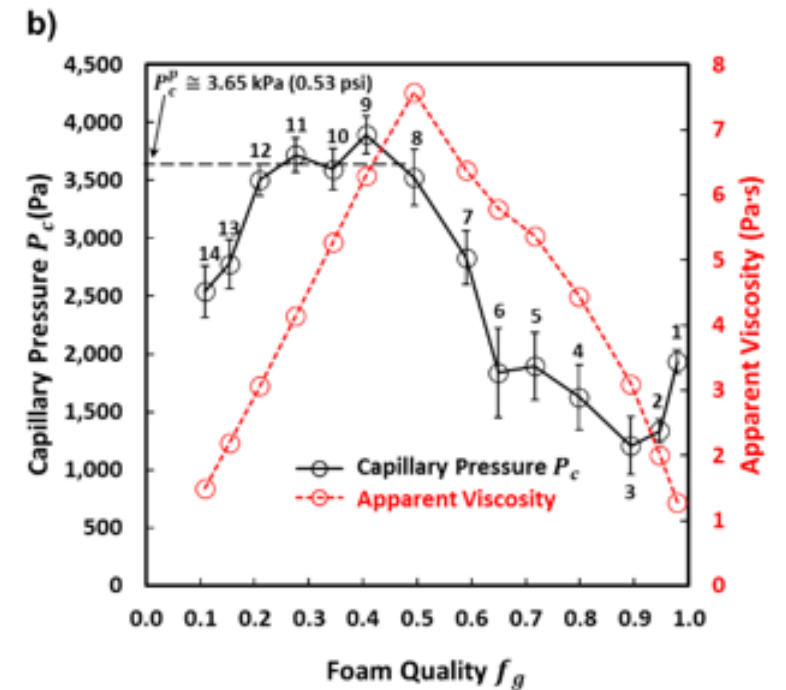
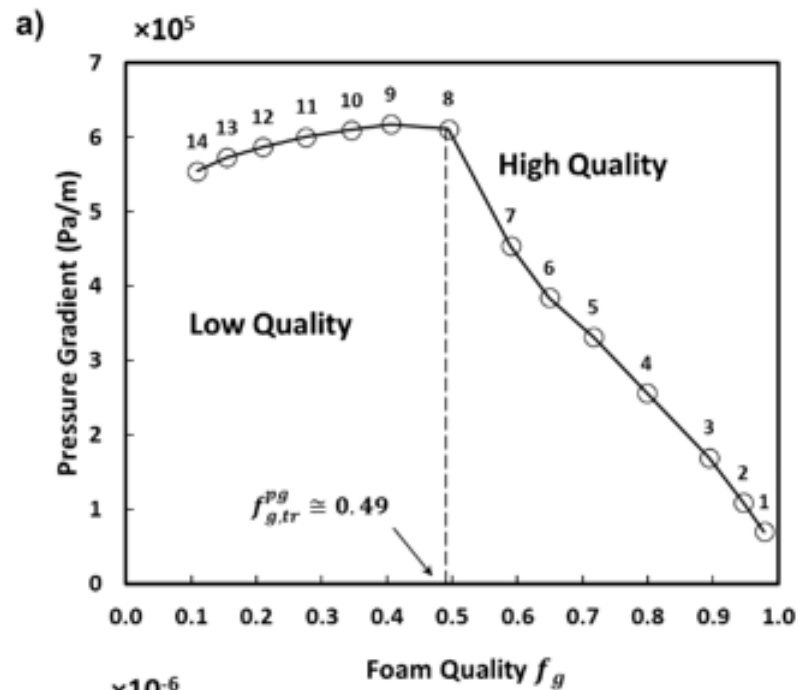


Fig. 12—Pressure drop during transient foam experiments with $f_g=67\%$ and $u_g=0.6$ ft/day in the heterogeneous (thick solid) and homogeneous (thin solid) columns. Arrows indicate the positions of gas front in the heterogeneous column at given times: (1) gas enters the fine sand section, (2) gas enters the coarse sand section and forms a strong foam front, (3) the strong foam front enters the last fine sand section, and (4) gas breaks through.

Foam apparent viscosity and capillary pressure as a function of foam quality, f_g

1% AOS 14-16
in 143 darcy sandpack,
Constant u_g

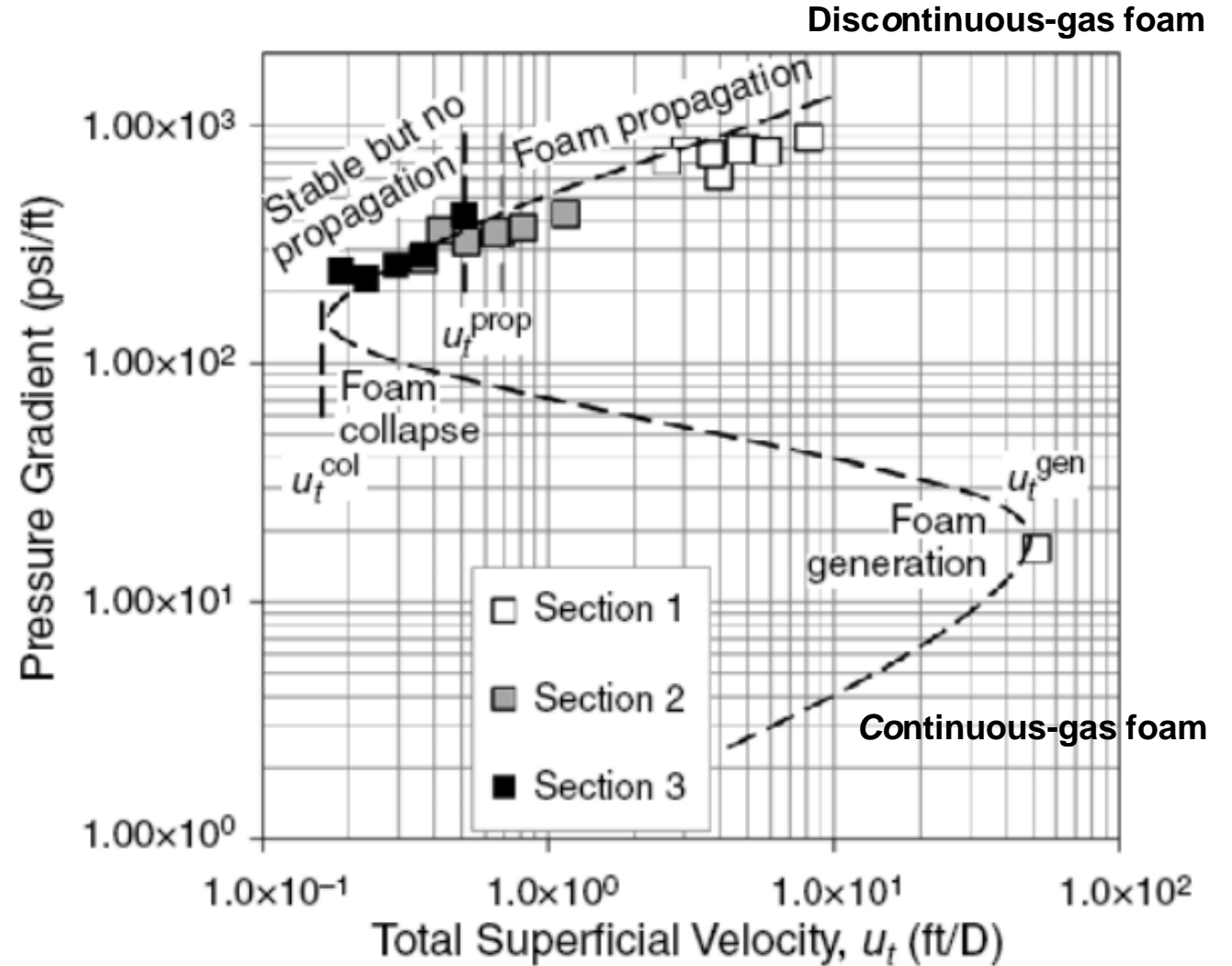
Vavra, et al., (2022), "Measuring In-situ Capillary Pressure of a Flowing Foam System in Porous Media", accepted *JCIS*.



Minimum pressure gradient for foam generation

Transition from continuous-gas foam to discontinuous-gas foam has a jump in pressure gradient when the minimum pressure gradient is exceeded.

$$f_g = 88\%, C_s = 0.3\%$$



(a)

Empirical foam model for reservoir simulation

- **CMG STARS foam model**
- **Gas mobility function of:**
 - Water saturation (S_w)
 - Velocity (Capillary Number)
 - Surfactant concentration
 - Oil saturation

Cheng, et al., 2000, SPE 59287
Zeng, et al., 2016, *Ind. Eng. Chem. Res.*, 55

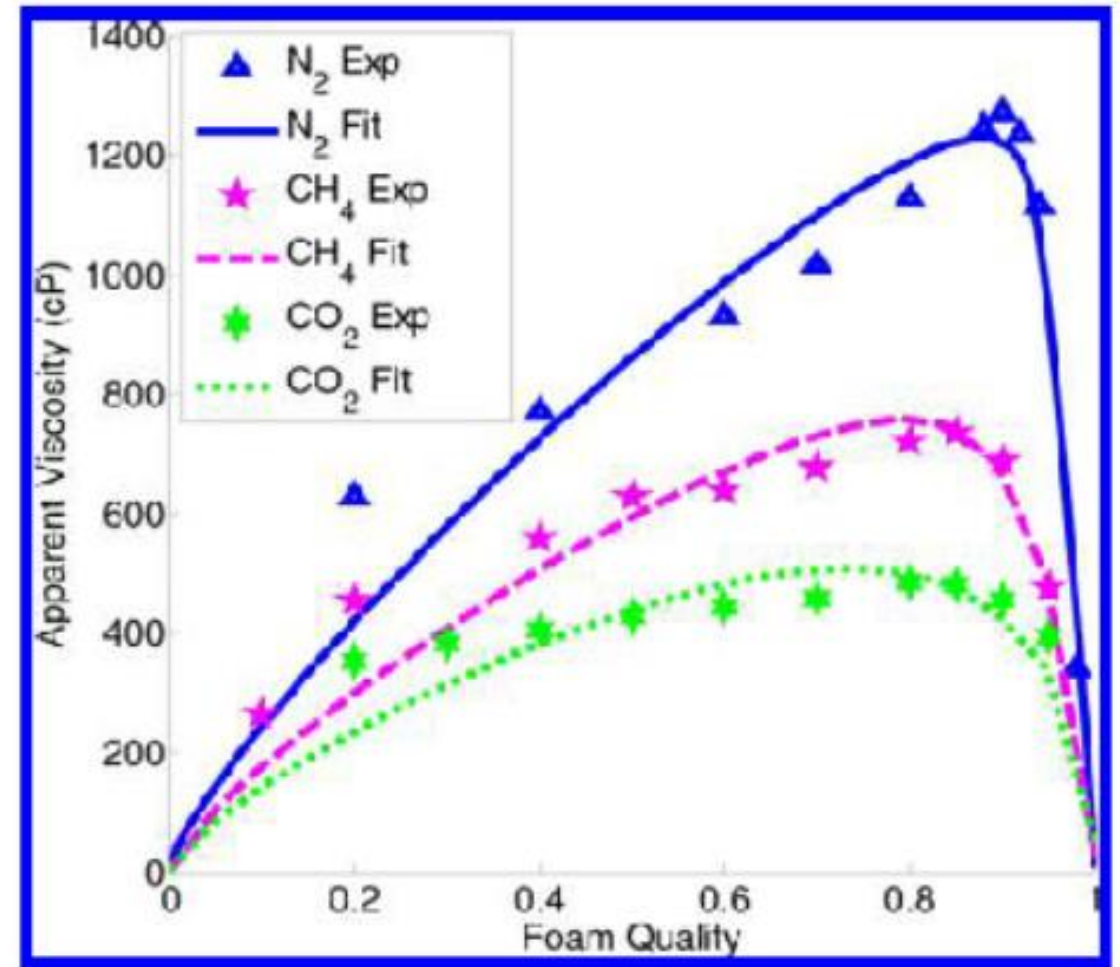
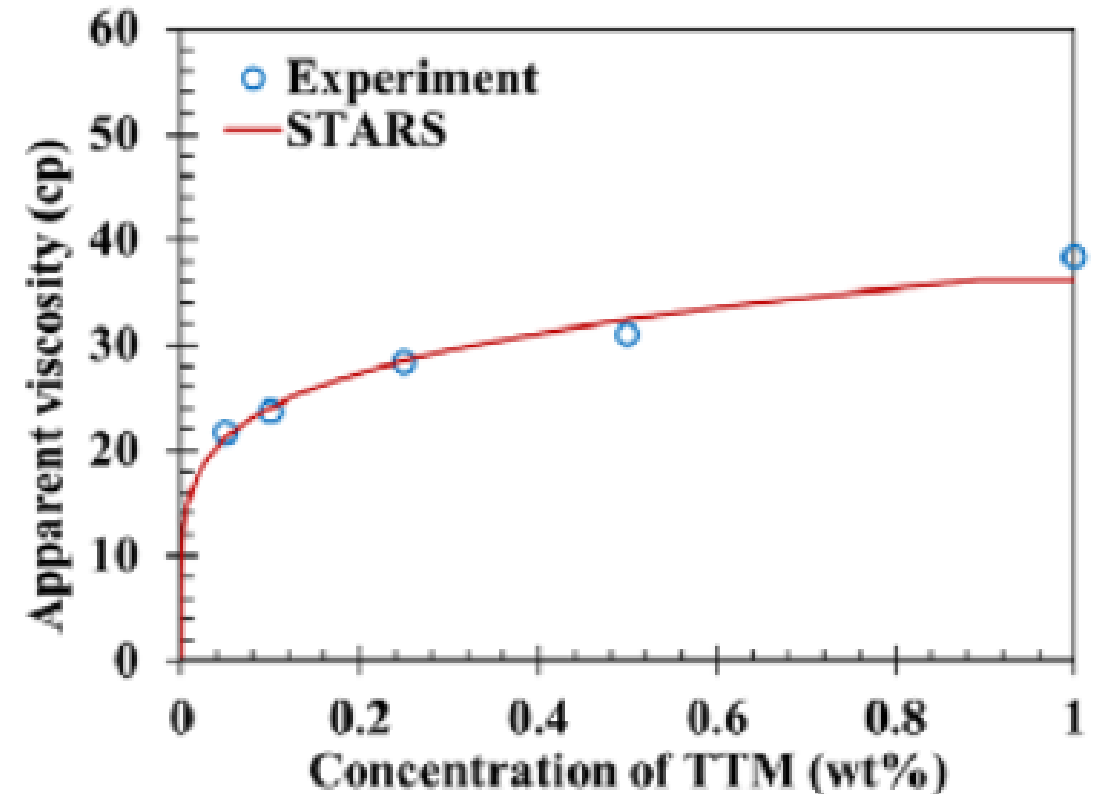
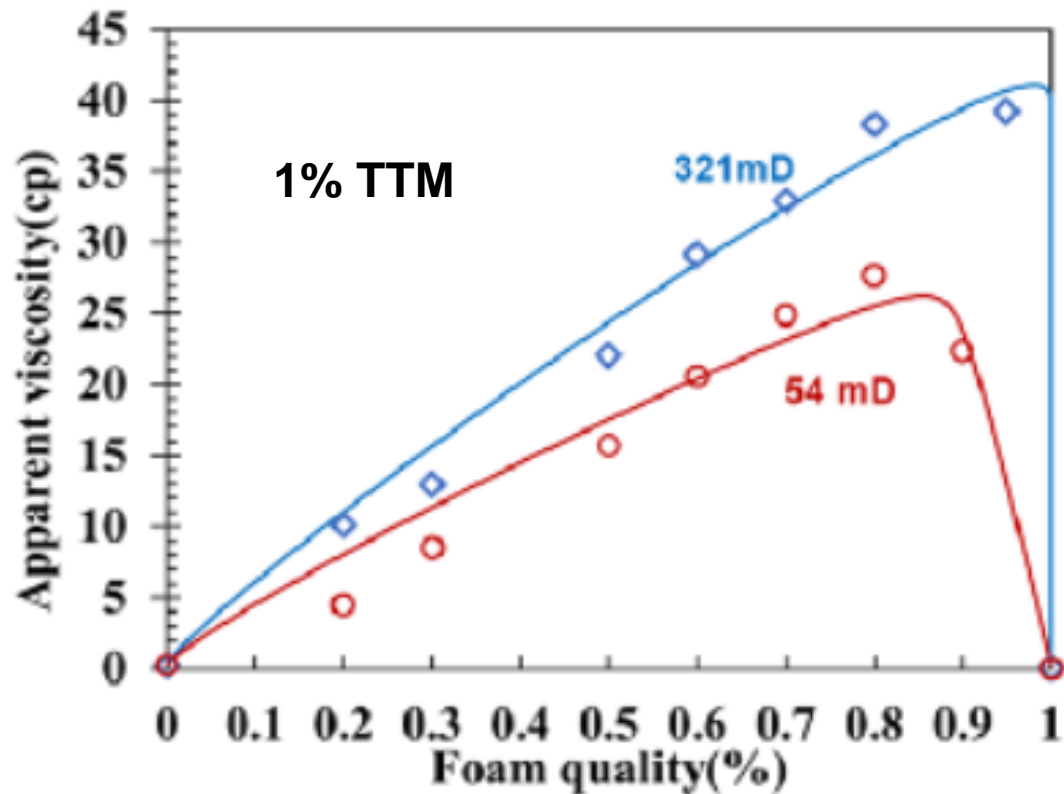


Figure 9. Data fit to STARS model for different gas type experiments.

Experiments for field application

Evaluation at: 120 °C, 3,400 psi CO₂, 22% TDS, limestone
TTM is a C16 – C18 diamine, cationic surfactant



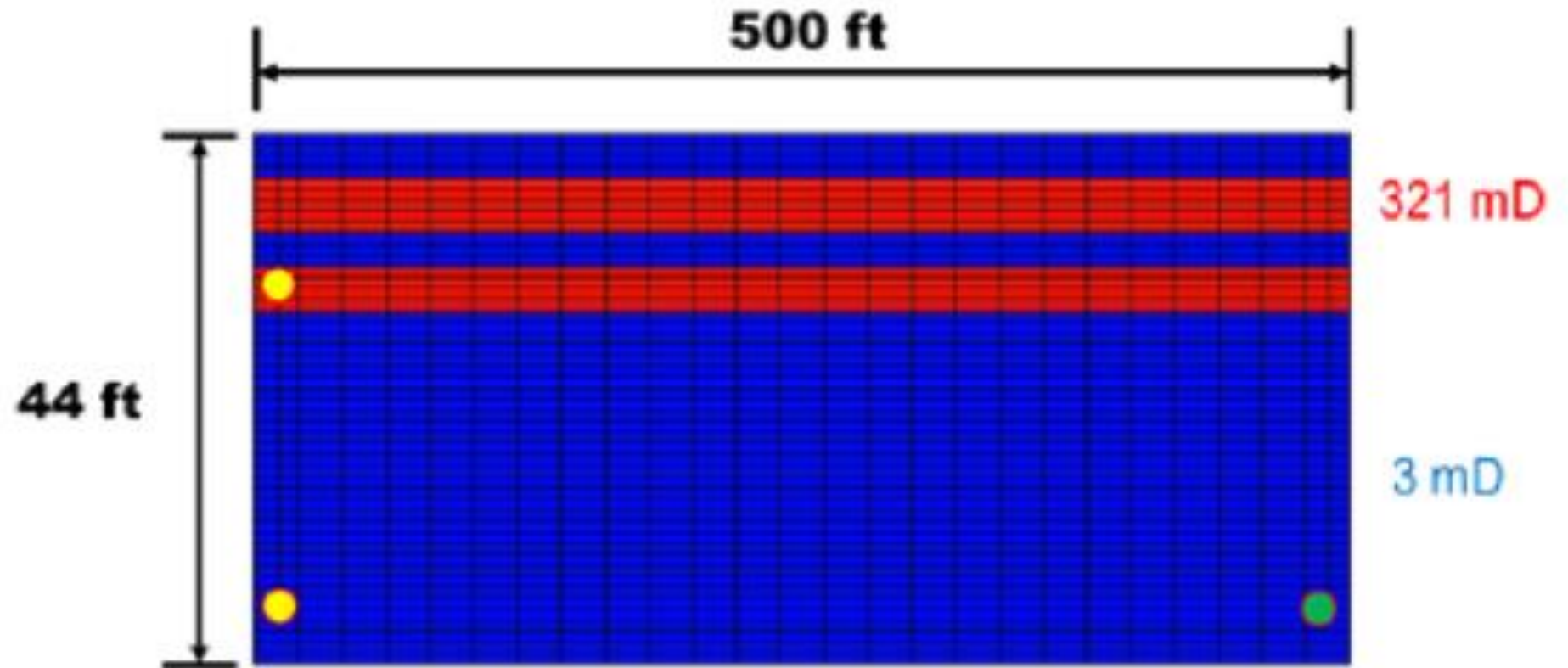
Simulations for field application

Cross-sectional view with horizontal wells

CO₂/TTM or CO₂/brine: upper left

CO₂ only lower left;

Producer; lower right

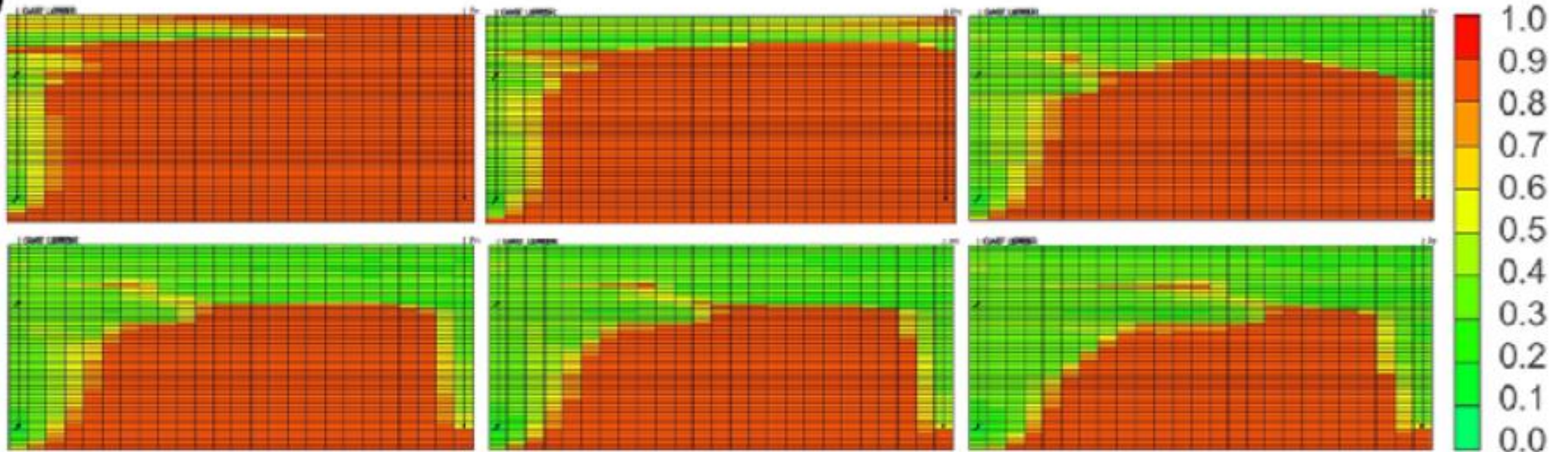


Simulations for field application

CO₂ & brine injection
1, 2, 5,
8, 10, 15 years

Oil
saturation

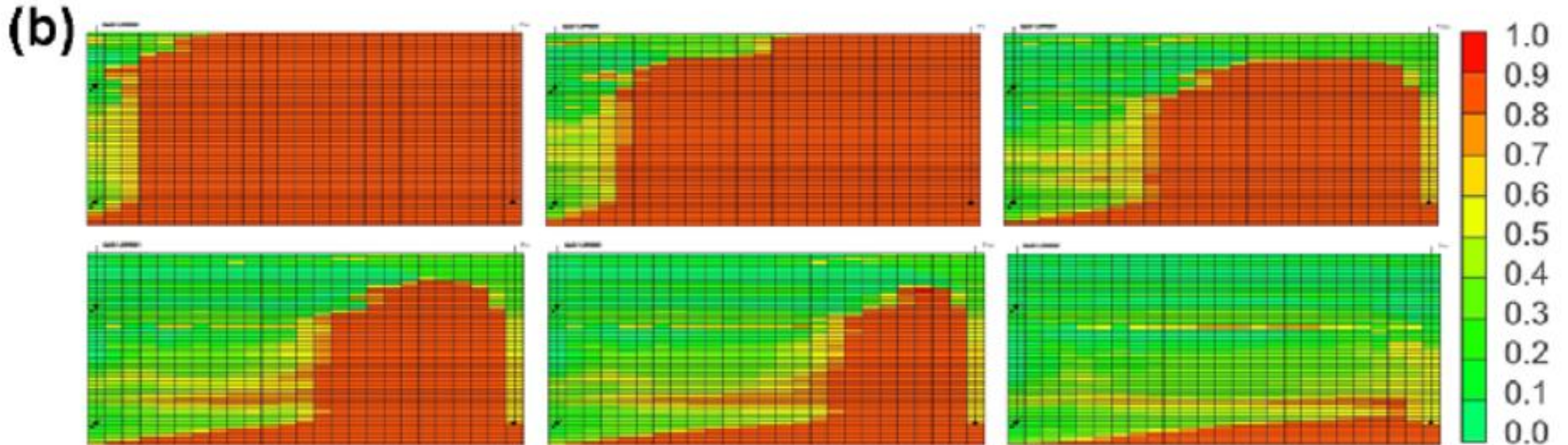
(a)



Simulations for field application

CO₂ & 1% TTM foam injection
1, 2, 5,
8, 10, 15 years

Oil
saturation



Conclusions

- **Choice of surfactant is essential**
- **Bubble size and distribution governs foam viscosity**
- **Bubble generation is governed by capillary heterogeneity and/or exceeding minimum pressure gradient**
- **Foam strength is limited by P_c and mass transfer**
- **Empirical models are available for fitting measurements and applying in simulators**
- **Reservoir simulators are available to evaluate benefit of foam mobility control for enhanced oil recovery**

References

- Chen, et al. (2015), "CO₂-in-Water Foam at Elevated Temperature and Salinity Stabilized with a Nonionic Surfactant with a High Degree of Ethoxylation," *I&EC Research*, 54, 16, 4252-4263.
- Cheng, L, et al., (2000), "Simulating Foam Processes at High and Low Qualities," SPE 59287, paper presented at 2000 SPE/DOE IOR Symp., 3-5 April.
- Elhag, et al., (2014), "Switchable diamine surfactants for CO₂ mobility control in enhanced oil recovery and sequestration," *Energy Procedia* 63, 7709-7716.
- Falls, A.H., et al., (1988), "Development of a Mechanistic Foam Simulator: The Population Balance and Generation by Snap-off," *SPE*, Aug., 884-892.
- Falls, A.H., Musters, J.J., and Ratulowski, J., (1989), "The Apparent Viscosity of Foams in Homogeneous Bead Packs," *SPE*, May, 155-164.
- Farajzadeh, R., et al., (2015), "Effect of Permeability on Implicit-Texture Foam Model Parameters and the Limiting Capillary Pressure," *Energy & Fuels*, 29, 3011-3018.
- Hirasaki, G.J., and Lawson, J.D., (1985), "Mechanisms of Foam Flow in Porous Media: Apparent Viscosity in Smooth Capillaries," *SPEJ*, April, 176-190.
- Jian, G., et al., (2020), "Evaluating the Transport Behavior of CO₂ Foam in the Presence of Crude Oil under High-Temperature and High-Salinity Conditions for Carbonate Reservoirs," *Energy & Fuels*, 33, 6038-6047.
- Svorstoel, I., et al., (1996), "Foam Pilot Evaluations for the Snorre Field," 8th European *IOR Symposium*, Vienna, Austria..
- Svorstol, I., et al., (1996), "Laboratory Studies for Design of a Foam Pilot in the Snorre Field," *SPE/DOE 35400*, Tulsa, OK.
- Tanzil, D., et al, (2002), "Mobility of Foam in Heterogeneous Media: Flow Parallel and Perpendicular to Stratifications," *SPEJ*, June, 203-212.
- Vavra, E., et al., (2022), "Measuring *In-situ* Capillary Pressure of a Flowing Foam System in Porous Media," *JCIS*, 621, 321-330.
- Yu, G., Vincent-Bonnieu, S., Rossen, W.R., (2020), "Foam Propagation at Low Superficial Velocity: Implications for Long-Distance Foam Propagation," *SPEJ*, Dec., 3457-3471.
- Zeng, Y., et al., (2016), "Insights on Foam Transport from a Texture-Implicit Local-Equilibrium Model with an Improved Parameter Estimation Algorithm," *Ind. Eng. Chem. Res.*, 55, 7819-7829.